Overview of investigations for Solar-Interplanetary-GeoMAgnetic storm connection

at Lab for Space Weather, Chinese Academy of Sciences

By Xueshang Feng and SIGMA Weather Team

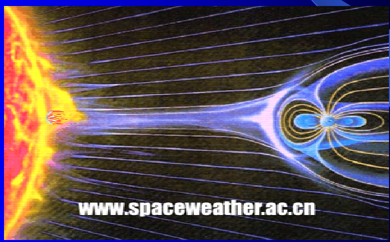

Contents

1、Propagation of Solar Storm

1.1 Interaction between CME and Structured Streamers

The asymmetrical propagation characteristics near the Corona is one of key factors in producing adverse space weather.

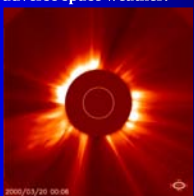

Wei and Dryer(Solar Physics 1991) have found: The solar disturbances induced by solar activities will have a tendency to deflect towards as well as focus on the heliospheric current sheet while propagating through the corona and interplanetary space, whether the eruptive sources are located at south or north hemisphere.

Numerical experiments can display this property. The asymmetric propagation features of CME event, triggered by two-D model with concentrically circular closed magnetic structure emeging at the solar northern latitudes 10 ° and 45 ° are simulated.

The numerical results show that magnetic structure has deflected to symmetrical line of CME. Magnetic field keeps deflecting to current sheet when it propagates outwards untill the center of MC propagates along the current sheet. (Sci in China) , This result is also in agreement with recent IPS data by Tokumaru et al, JGR, 2000.

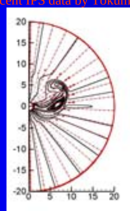

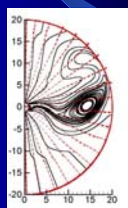

Numerical simulation for interaction between CME and streamer t=2.65 and 6.03Hrs (asymmetric center at theta=45 degree)

1.2 Numerical studies of coronal structures

In order to study the propagagtion, one of the important features is to construct pre-event corona.

Based on the solar observation, the coronal structure is numerically produced by 3D simulation.

•1998 May 1st event (Chin Astron & Astrophys)

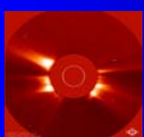

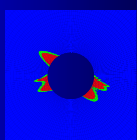

Left: LASCO observation, Right: Numerical result

• 1996.12 CME event（GRL）

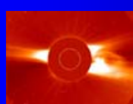

Left: LASCO observation, Right: Numerical result

•1999.8 CME event（GRL）

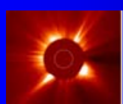

Left: LASCO observation, Right: Numerical result

1.3 Numerical study of Bz temperoal Behavior during 1997 Juruary Event(Sci in China)

In space weather event studies, the prediction of IMF Bz is very important. Using solar observation as inputs, the propagating process of January 1997 event is numerically simulated. The temporal Behavior of IMF Bz near the earth is shown to be in agreement with WIND data.

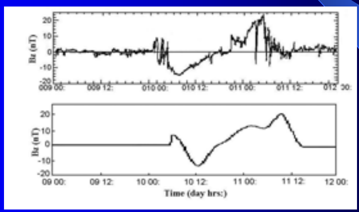

The temporal behavior of B_Z at 1AU (the upper one is the observation by WIND and the other is simulated result)

1.4 Propagation of other CME events(Advances in Space Research, Science in China)

Using 2D numerical model, the following CME events are numerically studied in interplanetary space.

- 1980.05.05 CME event
- 1980.08.18 CME event
- 1998.04.29 CME event

Example: 1998.05 CME

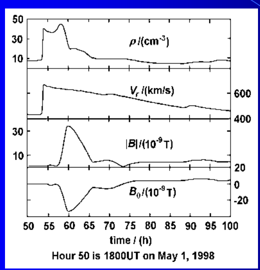

1.5 MHD Shock Jump Condition (Solar Physics）

•MHD shock jump conditions have been used for more than 50 years after Ruderman proposed in 1950;

We propose a new jump shock jump condition by introducing the shock manifold and combining jump condition of the normal derivatives and the plain jump conditions. In this way, a multi-step method for explosive shock waves in solar wind can be established and extend some classic results of shock theory;

The method provides a way of predicting the arrival of shock near the earth.

2、Numerical Schemes for the construction of MHD models

1) No free parameter, Non-oscillatory, Dissipative scheme (NND—A TVD Type)

2）Modified LAX-FRIEDRICHS-TVD scheme

3）Mixed GLM-MHD formulation method

2.1 Initial Boundary inputs

How to use limited solar observation as inputs to initialize the solar wind simulation in order to obtain realistic steady state solar wind is an important step in solar wind structure simulation. This kind of study can provide a realistic solar wind background for numerical space weather model.

In order to give a realistic initial boundary condition for numerical steady state solar wind model, a solar wind background model constrained to solar observations from WSO Magnetic observation and HAO K-coronal brightness are established such that three dimensional magnetic field, density and velocity can be properly obtained.

2.1.2 Example：Magnetic field, velocity and density for 1918CR

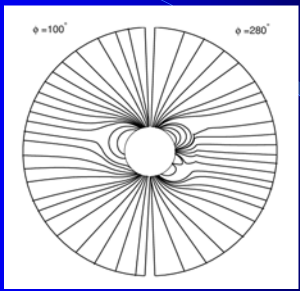

Meridional magnetic profiles at ϕ=280——100 degree from 1-5Rs

The latitudinal gradient of radial magnetic field Br on both sides of current sheet decrease with the increase of heliocentric distance，which are in agreement with Ulysses observation(μ T)

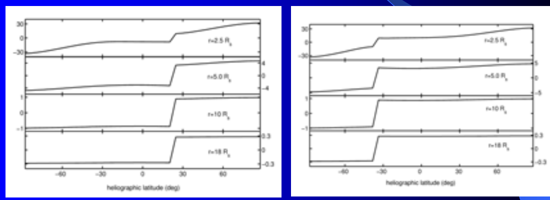

Br vs latitudes at ϕ=320 and 280 degrees

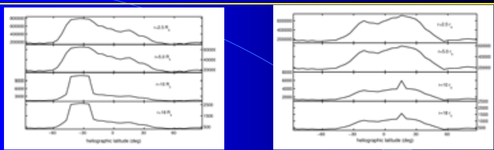

Number density (/cm^3) *vs latitudes at* ϕ=320和140 degrees

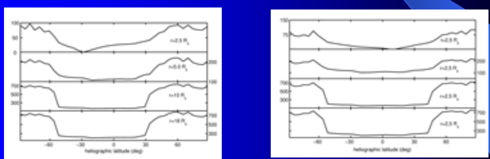

Radial velocity (Km/s) vs latitudes at ϕ=320 and 140 degrees

Velocity at current sheet is low while increases outside [-35,35] and afterwards no obvious change

2.2 Numerical simulation of steady solar wind for 1935CR

Using WSO 1935CR magnetic field observation as input, steady state 3D solar wind is simulated by modified Lax-Friedrichs MHD code

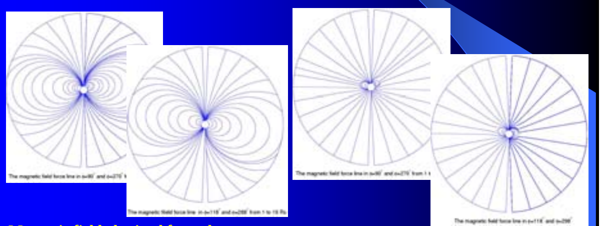

Magnetic field obtained from the photospheric magnetic field observation

Numerical steady results of magnetic field in meridian plane

3D Numerical results of magnetic field

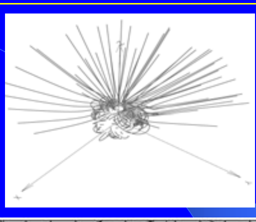

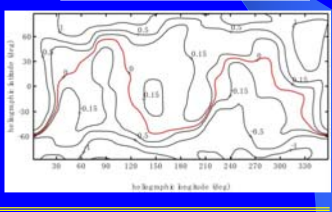

Simulated Magnetic filed structure at 2.5Rs，where red line is the current sheet(unit μ T)

Numerical number density： left 2.5Rs (10^5/cm^3);right 20Rs (10^2/cm^3)

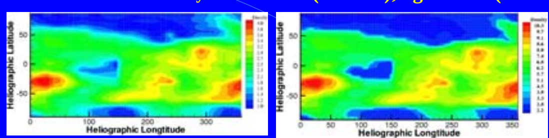

Vr (left) and density(right) vs radial

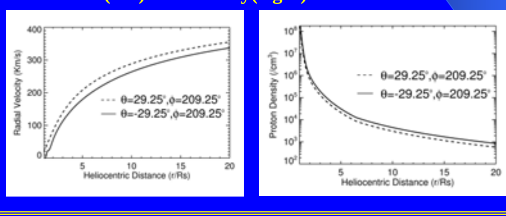

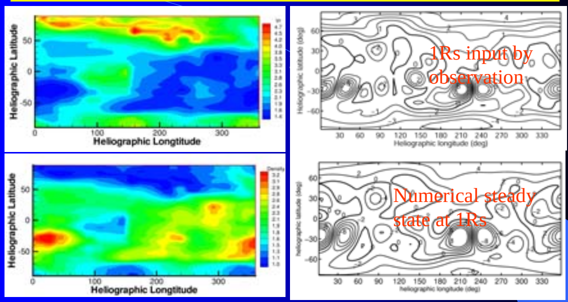

The importance of time-dependent boundary condition by non-reflective treatment

2. 3 Large scale structure of solar wind

To further validate our newly developed three-dimensional combined numerical MHD model of TVD Lax-Friedrich with MacCormack II together with calculation regional decomposition from 1 to 20Rs and 18Rs-1AU, the large scale structure of solar wind has been simulated by using the averaged data of Carrington Rotations 1888 to 1893 to determine the initial and boundary conditions .

Ulysses has been the first spacecraft to explore the high latitudinal regions of the heliosphere till now. During its first rapid pole-to pole transit from September 1994 to June 1995, Ulysses observed a fast speed flow with magnitude 700-800km/s at high latitudinal regions except at area near the ecliptic plane where the velocity is 300-400km/s. The observations also showed a sudden velocity jump across these two regions. Here, based on the observations of the solar magnetic field and a addition of the volumetric heating mechanism to the MHD equations, the large-scale solar wind structure mentioned above is reproduced by using a three-dimensional MHD model.

The numerical results are basically consistent with those of Ulysses observations. Our results also show that the distributions of magnetic field and plasma number density on the solar surface play an important role in governing this structure. Furthermore, the three-dimensional MHD TVD Lax-Friedrich numerical model used here has a robust ability to simulate this kind of large-scale wind structure.

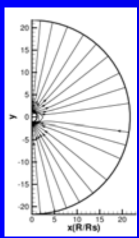

Computed magnetic field lines projected on the meridional plane at 42.75° (left) and at the 132.75° (right), respectively.

3D numerical result of magnetic field of north hemi-sphere.

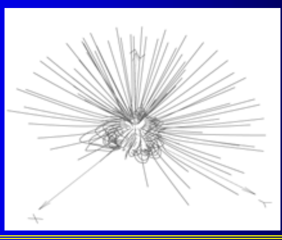

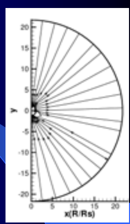

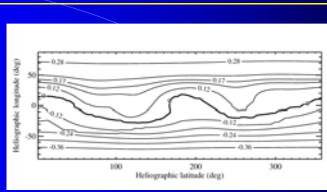

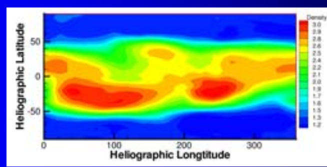

Computed contours of magnetic field (Gauss) and number (10^5/cm^3) density at 2.5Rs

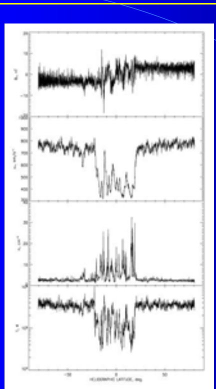

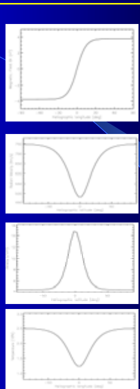

Left panel:

Observations by Ulysses

Right panel:

numerical results at 1AU (Br, Vr, N, T)

2.4 Mixed Generalized-Lagrange-Multiplier (GLM)-MHD formulation method

A new numerical scheme of 3rd order Weighted Essentially Non-Oscillatory (WENO) type for 2.5D mixed GLM-MHD in Cartesian coordinates is proposed. To show the validation and capacity of its application to MHD problem modelling, interaction between a magnetosonic shock and a denser cloud and magnetic reconnection problems are used to verify this new MHD code. It is significant to note that a new divergence cleaning approach for the MHD equations by coupling the divergence constraint with the evolution equations using a generalized Lagrange multiplier (GLM) is employed. The mixed hyperbolic/parabolic GLM ansatz offers both propagation and damping of divergence errors. Moreover, the magnetohydrodynamic part of the GLM-MHD system is still in conservation form by taking account of the arguments by Dellar and Dedner.

$$\frac{\partial}{\partial t}\begin{pmatrix}\rho\\ \rho\mathbf{v}\\ \mathbf{B}\\ U\\ \psi\end{pmatrix}+\nabla\cdot\left\{\begin{pmatrix}\rho\mathbf{v}\\ \rho\mathbf{v}\mathbf{v}+(p+\frac{1}{2}\mathbf{B}\cdot\mathbf{B})\mathbf{I}-\mathbf{B}\mathbf{B}\\ \mathbf{v}\mathbf{B}-\mathbf{B}\mathbf{v}+\psi\mathcal{I}\\ (U+p+\frac{1}{2}\mathbf{B}\cdot\mathbf{B})\mathbf{v}-(\mathbf{v}\cdot\mathbf{B})\mathbf{B}\\ c_h^2\mathbf{B}\end{pmatrix}^T\right\}^T=-\nabla\cdot\mathbf{B}\begin{bmatrix}0\\0\\ \mathbf{v}\\0\\0\end{bmatrix}+\begin{bmatrix}0\\ \mathbf{0}\\ \mathbf{0}\\ -\mathbf{B}\cdot(\nabla\psi)\\ -\mathbf{u}\cdot(\nabla\psi)-\frac{c_h^2}{c_p^2}\psi\end{bmatrix}$$

2.4.1 Two-D Orszag and Tang's MHD Vortex system

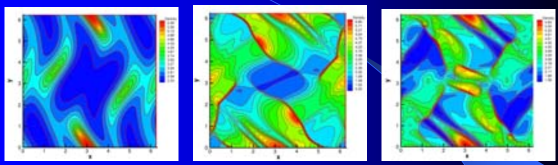

The density profiles : Left for density contours at $t=0.5$; Middle for density contours at $t=2$; Right for density contours at $t=3$

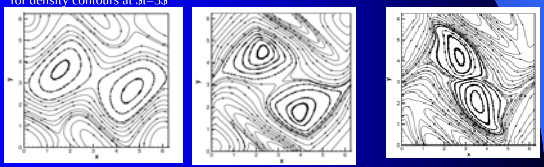

4.2 Interaction between a magnetosonic shock and a denser cloud

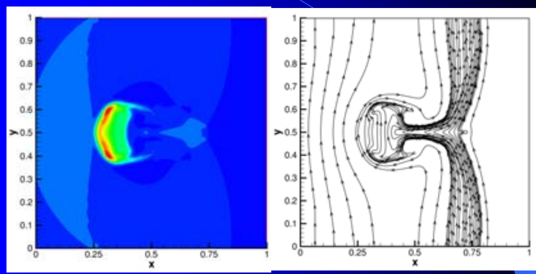

The interaction between a magnetosonic shock and a denser cloud: Left for mass density contours at t=0.06; Right for magnetic field at t=0.06.

4.3 Magnetic Reconnection

(plasma cloud at (0,6) with radius 0.5 and the computational domain with density five times higher than that of the background medium is driven with initial velocity $2 V_A$ (V_A Alfven velocity) towards the current sheet of the same form as that of \cite{weib}. The scenario is the typical interplanetary medium: $\beta=2.0 , R_m=2000, N_0=5/cm^3, T_0=1\times 10^5 K$.)

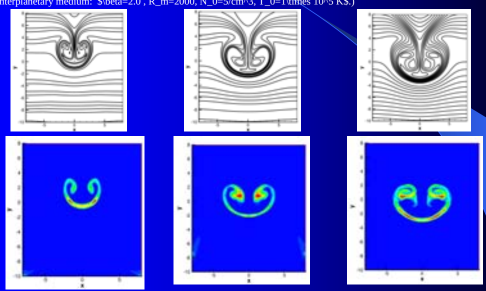

The magnetic field (upper panel) & density (low panel) profiles : Left at $t=10\tau_A$; Middle at $t=18\tau_A$; Right at $t=26\tau_A$.

The numerical tests for 2D Orszag and Tang's MHD vortex, interaction between a magnetosonic shock and a denser cloud and magnetic reconnection problems show that the third order WENO MHD solvers are robust and yield reliable results by the mixed GLM or the mixed EGLM correction.

Meanwhile, this method is very easy to add to an existing code since the underlying MHD solver does not have to be modified. It is worth noting that within our new approach divergence errors are transported by two waves with speeds independent of the fluid velocity.

This treatment has been used by us to our former solar wind models and the obtained numerical results are encouraging in keeping Div(B)-free.

3、Studies of fundamental physical mechanisms between Sun-Earth system

3.1 Boundary Layer of IMC (J.G.R, G.R.L)

Based on a statistical analysis of the boundary physical states of 80 magnetic clouds reported in the literature from the years 1969 to 2001, we suggest a new identification of the magnetic cloud boundary by describing it as front and tail boundary layers (BLs) formed through the interaction between the magnetic cloud and the ambient medium.

The outer boundary of the layer often displays the properties of magnetic reconnection, which could be characterized by a ‘‘three-high state’’ (relatively high proton temperature, high proton density, and high plasma beta) and the corresponding magnetic signatures (the magnetic intensity drop and the directions change abruptly: the abrupt azimuthal changes, delta(phi)~180, and latitudinal changes, delta(theta)~90, in the magnetic field).

The inner boundary of the layer exhibits a ‘‘three-low state’’ (relatively low proton temperature, low proton density, and low plasma beta) and separates the magnetic cloud body, which has not basically been affected by the interactions, from the boundary layers.

The front boundary layer could be associated with the outer loops of CMEs and its average time scale is 1.7 hours; the tail boundary layer seems not be a filament and its average time scale is 3.1 hours. The distribution function of magnetic fluctuations in the boundary layer is significantly different from those in the ambient solar wind and the cloud body itself. The preliminary numerical simulation in principle confirms this new identification and could qualitatively explain most of the observations of the cloud boundary.

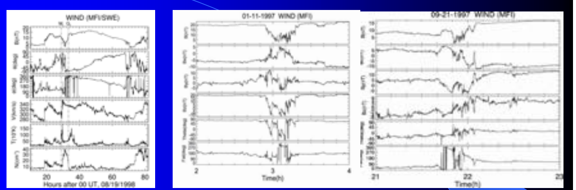

Examples: Boundary layer of interplanetary magnetic cloud (M_f, G_f) and shock、sheath and magnetic cloud body (left)

Magnetic cloud boundary layer (right)

3.2 possible mechanism of MC boundary layers(J.G.R）

MC boundary layers may be produced by magnetic reconnection. This mechanism can explain the basic observations of MC and is principally produced by numerical simulation. At the outer boundaries, magnetic strength decreases abruptly, its directions also changes abruptly(△Φ~180°,△θ≥45°）and have three high states: high density、high temperature、high plasma beta，at the inner boundary, magnetic strength increases、its directions change gradually and have three low states:：low density、low temperature and low plasma beta.

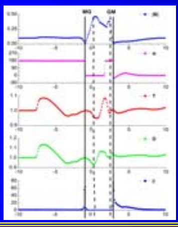

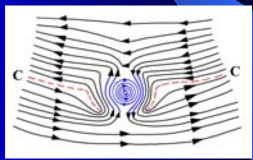

Sketch mechanism for formation of IMC（Left）& numerical simulation（right）

3.3. Small scale turbulent magnetic reconnection (Space. Sci Rev., Sci in China, Chin Sci Bulletin)

Using Helios data, it is found that turbulent magnetic reconnection may exist in solar wind.Based on a high accurate resolution compact upwind numerical scheme, small scale magnetic reconnection problem is numerically studied for high Reynold number Rm＝2000-10000.

- The simulated results show that the magnetic reconnection process could occur under the typical interplanetary conditions. These obtained magnetic reconnection processes own basic characteristics of the high *Rm* reconnection in interplanetary space, including multiple X-line reconnection, vortex velocity structures, filament current systems, splitting, collapse of plasma bulk, merging and evolving of magnetic islands, and lifetime in the range from minutes to hours, etc. These results could be helpful for further understanding the interplanetary basic physical processes.

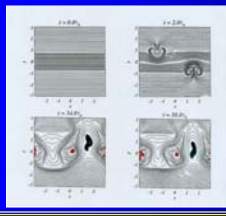

Magnetic field evolution (R_M=10000)

3.4 Global structure of coronal mass flux output and magnetic field(J.G.R)

The basic characteristics of the coronal mass output near the Sun are analyzed with the statistic and numerical methods by using observational data from K corona brightness, IPS(interplanetary scintillation), and photospheric magnetic field during the descending phases (1983) and the minimum (1984) of solar activity from the point of view of the global distribution of the solar magnetic field on the source surface (at 2.5 solar radii (Rs)).

The main results are as follows: (1) There are certain regular persistent patterns in the global distributions of coronal mass outputs flux Fm (density x speed V), which shows that the highest Fm in 1983 and 1984 display more regularly double peaks and single-peak wave-like patterns on the source surface (2.5 RS), respectively. The highest and the lowest Fm are associated with the coronal current sheet and the polar corona regions, respectively, and the other regions are associated with a moderate Fm. (2) The speed dependence of Fm is different for various magnetic structures.

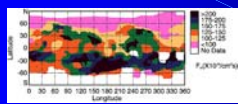

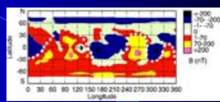

Statistic results: (left)The global distribution of the coronal mass flux output Fm on the source surface at 2.5 Rs during the Carrington rotations 1733–1742 in 1983. (right)Global distribution of the magnetic field strength, B(nT), on the solar photosphere averaged over the same period. The interfaces indicate the positions of the neutral line regions. For comparison the large-scale envelope of neutral line regions on the photosphere is also plotted here (white circles).

By solving a self-consistent MHD system based on the observations of K coronal brightness and the photospheric magnetic fields, a

preliminary numerical study of the global distribution near 2.5 Rs for the Carrington rotation 1742 in 1983 has been made.

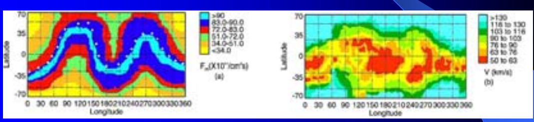

Numerical results of Fm(left), speed on the source surface (2.5 Rs)(right) for the Carrington rotation 1942 in 1983. They are obtained from the MHD model with the observational data of the photospheric magnetic fields and K coronal brightness as inputs.

4、Solar disturbances & geomagnetic storm prediction: statistical methods

4.1 Geomagnetic disturbance ISF prediction method(Adv Space Res, Sci in China)

Based on a combined approach of solar activity, interplanetary scintillation (I) and geomagnetic disturbance observations during the period 1966-1982 together with the dynamics of solar wind storm propagation (S) and fuzzy mathematics (F), a ISF prediction method is proposed.

For prediction tests for 37 geomagnetic disturbance events during the descending solar activity phase 1984-1985, we have.

For the onset time of the geomagnetic disturbance, the relative error between the observation, T_{obs}, and the prediction, T_{pred}, $\Delta T_{pred}/ T_{obs}$ <10% for 50% events，< 20% for 70% events; (图：地磁扰动渡越时间预报的相对误差(N, ΔT/T)

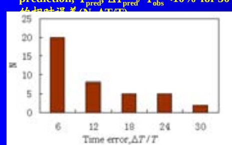

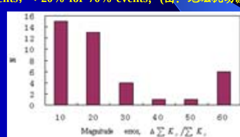

(2) for the magnetic disturbance magnitude, the relative error between the observation, $\Sigma K_{p,\ obs}$, and the prediction, $\Sigma K_{p,\ pred}$, $\Delta\Sigma K_{p,\ pred}/ \Sigma K_{p,\ obs}$ < 30% for 80% events，> 60% for only 15% events (图：地磁扰动幅度预报的相对误差(N, ΔKp/Kp)

This shows that the prediction method described here has encouraging prospects for improving predictions of large geomagnetic disturbances in space weather events.

6

4.2 Solar wind parameters prediction-SSP method (JGR)

Based on K-coronal brightness and photospheric magnetic field as inputs, a simplified MHD method is proposed to obtain the solar surface parameters at 2.5 Rs and then empirical relation is used to derive the solar wind parameters near the earth(Source Structure Prediction Method, SSP method).

Example: The predicted temperature and radial velocity near the earth for 1742CR 1983

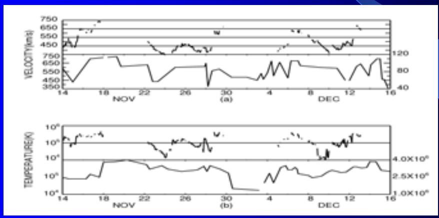

The predicted results(lower) compared with IMP8 observation(upper) The right ordinate stands for the values at 2.5 RS and the left ordinate for the values neart the earth.

CAWSES Beijing

4.3 Modified Shock Propagation Method(MSP) for prediction of shock arrival time at 1AU

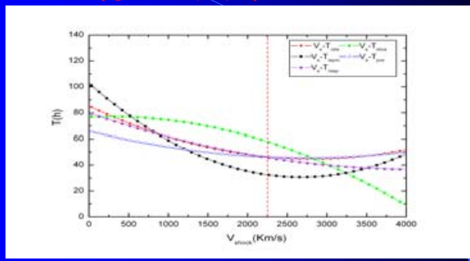

97 events: Observation→red; STOA→green, ISPM model→black dot, our former model→triangle, MSP model→ ?

CAWSES Beijing

Thanks !